Published in final edited form as:

J Mater Chem B. 2014 May 28; 2(20): 3107–3114. doi:10.1039/c4tb00287c.

Ultrabright NIR fluorescent mesoporous silica nanoparticles†

S. Palantavida[a], **R. Tang**[b], **G. P. Sudlow**[b], **W. J. Akers**[b], **S. Achilefu**[b,c], **I. Sokolov**[a,d,e]

[a]Departments of Mechanical Engineering, Tufts University, Medford, MA 02155, USA

[b]Departments of Radiology, Washington University, St. Louis, MO 63110, USA

[c]Departments of Biomedical Engineering, Washington University, St. Louis, MO 63110, USA

[d]Departments of Biomedical Engineering, Tufts University, Medford, MA 02155, USA

[e]Departments of Physics, Tufts University, Medford, MA 02155, USA

Abstract

Near-infrared (NIR) water-dispersible fluorescent tags are of big importance for biomedical imaging. Bright, stable, biocompatible NIR fluorescent nanoparticles have great translation potential to improve diagnosis of early stages of different diseases. Here we report on the synthesis of exceptionally bright ("ultrabright") fluorescent meso(nano)porous silica nanoparticles of 28 ± 3 nm in diameter. The NIR fluorescent dye LS277 is encapsulated inside these silica nanoparticles. The wavelengths of the maximum excitation/ fluorescence of the particles are 804/815 nm. The absorptivity coefficient of the particles is 2.1×10^8 M^{-1} cm^{-1} at 805 nm and the quantum yield of the dye increased by a factor of 5 after encapsulating to 1.5%. The fluorescent brightness of these particles is more than 2000× higher than the fluorescence of one molecule of LS277 in water. When exited in NIR spectral region (>700 nm), these particles are up to 4× brighter than QD800 commercial quantum dots emitting at 800 nm. We demonstrate that the synthesized NIR mesoporous silica nanoparticles easily internalize 4T1luc breast tumor cells, and remain bright for more than 9 weeks whereas the dye is completely bleached by that time.

Introduction

Silica-based nanoparticles present an excellent platform for biomedical imaging and therapy because of their biocompatibility and ability to carry payloads, including contrast agents and drugs.[1] In particular, silica nanoparticles can be produced economically and are size-tunable with easy surface conjugation chemistry.[2,3] These factors are important in optical molecular imaging, enabling loading of organic fluorescent dyes and high affinity surface ligands. When functionalized with sensing molecules, the particles can be used to label and track specific molecular processes, biomolecules, cells, and tissues of interest *in vitro* and *in vivo.* For example, quantum dots (QDs), one of the brightest types of fluorescent nanoparticles, have been used to demonstrate successful *in vivo* imaging of molecular signatures in animal

†Electronic supplementary information (ESI) available: DLS size distribution results, quantum yield and life-time measurements. See DOI: 10.1039/c4tb00287c

igor.sokolov@tufts.edu; achilefus@mir.wustl.edu.

cancer models.[4–6] Fluorescent nanoparticles can be conjugated with multiple biomolecules for multimodal, multiplexed imaging of specific processes, molecules, cells, and tissues.[7–11]

Due to a relatively deep tissue penetration and low tissue autofluorescence in the near-infrared (NIR) region between 700 and 900 nm, NIR fluorescent dyes are attractive in modern optical imaging of biological targets *in vivo*.[12] The number of organic NIR fluorophores has expanded significantly in recent years, but suffer from relatively low quantum yield compared with visible wavelength fluorophores. More recently, NIR fluorescent QDs have been developed for *in vivo* imaging. However, a number of lingering concerns such as toxicity and stability of NIR QDs mitigate the potential translation of QDs to humans.[13] NIR dye-doped stable polystyrene nanoparticles were recently reported and used to image cells.[14] Higher NIR fluorescent brightness of nanoparticles is much needed to detect smaller and deeper tagged regions in the human body *in vivo*. Bright, stable, biocompatible NIR fluorescent nanoparticles have great translation potential to improve diagnosis of early stages of different diseases, including cancer, in which early detection can substantially decrease mortality due to this disease.

Incorporation of fluorescent dyes in nanoscale structures is another method of making fluorescent nanoparticles. For example, there have been many attempts to make fluorescent nanoparticles silica of high brightness.[15–22] Most of these approaches utilized the covalent coupling between fluorescent dye and silica. Recently, the use of tris(2,2A-bipyridyl)dichlororuthenium(II) hexahydrate (Rubpy) dye was reported to non-covalently dope silica nanoparticles.[23] All of these particles showed brightness comparable with a single bright quantum dot at best.

Novel ultrabright meso(nano)porous silica particles of micron-size[24–27] and nano-size[2,3,28] have been recently reported. The key difference with the previous methods was that organic fluorescent dyes were non-covalently (just physically) entrapped inside nanochannels of these particles. Due to the physical encapsulation and specific nano-environment (the presence of alkane chains of templating molecules), the dyes did not lose its fluorescent activity up to rather high concentrations which were reached inside the particles. As was shown, the particles loaded with rhodamine dyes (for example, rhodamine 6G dye, 525 nm maximum absorbance, 550 nm maxim emission in water) possessed fluorescence higher by three-four orders of magnitude compared to the maximum fluorescence of free dye in the same volume in water. Encapsulation of dyes within the nanoporous silica nanoparticles did not show the evidence of quenching that is typically seen at these high concentrations. The quantum yield of the encapsulated dye stays unchanged. And the same time the extinction coefficient of the particles increases several hundred times compared to the individual dye molecules. It makes the fluorescence of the particles “ultrabright”. It was shown[2] that nanoparticles of 20–50 nm in diameter have brightness equivalent to the fluorescent brightness of up to 770 molecules of RG6 dye. This makes the particles brighter than the brightest quantum dots (when compared to the same emission/excitation wavelengths) of similar size (water-dispersible, *i.e.*, coated quantum dot of the same fluorescent spectra as R6G dye have the diameter of 13–30 nm (ref. 6 and 29)). Unfortunately, the spectral range of these particles has not been conducive to deep tissue imaging, and encapsulation of NIR dyes in mesoporous silica nanoparticles has not been reported.

The most common biocompatible NIR dyes are the polymethine cyanine dye family, comprising benzoxazole, benzothiazole, indolyl, 2-quinoline and 4-quinoline subclasses.[30] These dyes have adjustable optical properties and high extinction coefficients (>150 000 M^{-1} cm^{-1}). The quantum yields of many NIR polymethine dyes are typically less than 15% in aqueous environment and sensitive to photobleaching. The development of NIR dyes with high quantum yield has to compensate for the energy gap law,[31,32] which anticipates low fluorescence efficiency. A new class of NIR dyes with a relatively high quantum yield in the NIR region has been recently reported,[33,34] but is poorly soluble in water. Dyes with good quantum yield in non-polar media generally demonstrate lower quantum efficiency in aqueous environments.[35] However, NIR absorbing cyanine dyes still have a lot advantages as biomedical optical probes because of their optimal spectral, chemical and biological properties as well as excellent safety profile of indocyanine green dye in humans.

Here we demonstrate that it is possible to create ultrabright silica nanoparticles using polymethine cyanine dye LS277, which is suitable for the use in microscopy and deep tissue imaging. 28 ± 3 nm size particles were synthesized. The wavelengths of the maximum excitation/fluorescence of the particles are 804/815 nm. The extinction coefficient of the particles $\varepsilon = 2.1 \times 10^8$ M^{-1} cm^{-1} at 805 nm and the quantum yield of the dye increased by a factor of 5 after encapsulating to 1.5%. This makes each particle more than 2000× fluorescently brighter than one molecule of LS277 in water. We demonstrate that the synthesized NIR silica nanoparticles easily internalize 4T1luc breast tumor cells, and remain fluorescent substantially longer compared to free dye.

Results and discussion

Two samples with two different LS277 dye concentrations were synthesized: NP1_LS277 (0.017 molar part of LS277, see the Experimental section) and NP2_LS277 (0.0026 molar part). The uniformity and narrow size distribution of the nanoparticles (NP-dye construct) were demonstrated through a combination of DLS measurement (ESI, Fig. S1†) and TEM images, (Fig. 1). The DLS measurement showed that these nanoparticles have an intensity-averaged hydrodynamic diameter of 28 ± 3 nm for both samples. The TEM images revealed a porous structure of the particles and their close-to-spherical shapes. The particle size seen in the TEM images comparable to the one measured with the DLS technique. Both NP1_LS277 and NP2_LS277 are identical in size within the error of measurements.

The absorbance and fluorescent spectra of the LS277 dye and silica nanoparticles with the dye encapsulated are shown in (Fig. 2). The comparison between free and encapsulated (inside the particles) dyes revealed a slight red-shift of *ca.* 10 nm occurred for both the maximum absorption peak at 804 nm and emission peak of 815 nm. (The maximum absorbance of free dye in water was 0.31 (1.2×10^{-5} M concentration) and 0.011 for the particles (0.02 mg mL^{-1})). This is presumably related to the change of LS277 environment before and after encapsulation into the porous matrix of silica nanoparticles, which includes

†Electronic supplementary information (ESI) available: DLS size distribution results, quantum yield and life-time measurements. See DOI: 10.1039/c4tb00287c

the interaction with silica matrix and confining by the alkane chains of the surfactant molecules.

Fluorescent brightness of the particles depends on the concentration of the dye molecules encapsulated, quantum yield of the dye, its extinction coefficient, dye association and aggregation, and the scattering of excitation light by the particles. At high concentrations in water, the dye molecules associate to form aggregates, which quench fluorescence and decrease overall brightness. To measure the brightness of the synthesized particles, we use the units broadly utilized in flow cytometry, MESF units (Molecules of Equivalent Soluble Fluorochrome). This measure is robust and virtually instrument independent. It was used to characterize brightness of fluorescent particles in ref. 1, 6, 23, 36 and 37. Briefly, the idea of the method is in finding the brightness of individual particles relative to the fluorescent brightness of individual dye molecules. Using LS277 as the reference dye, and measuring fluorescence coming from the solution with known concentrations of fluorescent silica nanoparticles C_{NP} and the reference dye C_{LS277}, one can find the sought relative brightness of a single nanoparticle (or brightness in MESF units, see the above) as follows

$$\text{Relative brightness} = (FL_{NP}/C_{NP})/(FL_{LS277}/C_{LS277}), \quad (1)$$

where FL_{NP} (or C_{LS277}) is the amount of fluorescent light coming from a suspension of the particles in water (or solution of reference LS277 dye). Because the spectra of both nanoparticles and LS277 dye are all the same, FL can either be the value of measuring fluorescence at a particular wavelength, or the integral over the emission wavelength interval.

For the example of NP1_LS277 particles, the relative brightness was calculated as follows. The concentration of NP1_LS277 particles in water was found to be 1.9×10^{13} particles per mL (it was measured by weighing the particles dried from the particle's water suspension, see the ESI†). This produced the integral fluorescence of 950 au. The concentration of LS277 dye in water was found to be 7.5×10^{-5} M (the concentration was calculated from the absorbance, see the ESI†), or 4.5×10^{16} molecules per mL, which produced the integral fluorescence of 1100 au. This will give 2070 fold for the relative brightness of nanoparticles. Taking into account the errors in measurements of the above parameters, we can arrive at the relative brightness of NP1_LS277 nanoparticles equal to 2070 ± 40 brightness of individual LS277 molecules (MESF units). Similar measurements done for NP2 particles give the value of 630 ± 50 for the relative brightness of NP2_LS277 nanoparticles.

Although being presumably the simplest and robust definition of brightness, eqn (1) is not commonly used for standard fluorophores. More basic quantities are typically used to describe the fluorescent "power" of fluorophores; the quantum yield and the extinction coefficient (or the cross-section). The relative brightness is then proportional to the quantum yield times the extinction coefficient. This definition is broadly used for molecular fluorophores and quantum dots[13] because those cannot be considered as consisted of multiple fluorophores. When considering fluorescent particles carrying fluorescent dye, this definition may become ambiguous. Let us demonstrate it. Eqn (1) can be continued as follows:

$$\begin{aligned}&\text{Brightness of nanoparticle} = \text{MESF}\\&\times \text{brightness of 1 molecule of LS277}\\&= Q_{\text{free LS277}} \times \varepsilon_{\text{free LS277}} \times N_{\text{effective of LS277}}\\&= Q_{\text{encapsulated LS277}} \times \varepsilon_{\text{encapsulated LS277}}\\&\times N_{\text{encapsulated LS277 molecules}} \equiv Q_{\text{particle}} \times \varepsilon_{\text{particle}}\,.\end{aligned} \tag{2}$$

Here MESF is Molecules of Equivalent Soluble Fluorochrome (number of LS277 molecules in this case), Q is the quantum yield, ε is the extinction coefficient (absorptivity), and N is the number of molecules of fluorophore molecules inside one particle. The last part of this equation is the definition of "quantum yield of the particle" (Q) and its extinction coefficient. There is an ambiguity where to assign the change of the quantum yield and the extinction coefficient of the encapsulated dye, either to the quantum yield or the extinction coefficient of the particle. This is nontrivial because of the scattering of light by the particle surface. The scattered photons of the exciting light do not reach the encapsulated dye, and consequently, do not produce fluorescence. It is a matter of semantic to assign this to the effective decrease of the quantum yield of the particle or to the extinction coefficient. To avoid this ambiguity, the definition given by eqn (1) is typically used when dealing with particles containing molecular fluorophores. To avoid confusion of these two definitions, the definition of eqn (1) could be called "apparent relative brightness". Furthermore, we conceived that it is more informative to measure the change of quantum yield of the fluorescent dye after encapsulation rather than to introduce "the quantum yield of the particles". This is what was done in our previous works.[2,3,26–28,38]

It is instructive to verify our measurements with respect to possible quenching of fluorescence of dye molecules, which are located in close proximity from each other inside the particles. Due to the hydrophobic nature of dye LS277, the dye itself has a relatively poor solubility in water and tends to aggregate. Low fluorescence was observed for LS277 dye molecules in water, which attributes to self-quenching *via* non-radiative energy transfer mechanism (homo-FRET) between fluorophores in close proximity. As we described previously, the unique pore architecture inside the particles synthesized here prevented aggregation of dye even at high concentrations.[2,3] Here we check that the distance between the molecules of LS277 is consistent with the lack of self-quenching.

Self-quenching can be estimated by calculating the Forster distance of a homo FRET pair (R_0). If the distance between molecules encapsulated in the silica is larger than R_0, the selfquenching is small. R_0 can be found using a known FRET calculator[39] which requires the knowledge of steady-state absorption and emission spectra of the dye as follows:

$$R_0 = 0.211\left(k^2 n - 4\Phi_{\text{d}} J(\lambda)\right)^{1/6}\ \text{Å}\,, \tag{3}$$

where k^2 is the orientation factor equal to 2/3 for randomly oriented fluorophores; n is the refractive index assumed to be 1.4 for organic molecules in aqueous solutions; Φ_{d} is the quantum yield of the donor; $J(\lambda)$ is the spectral overlap integral. Using spectra shown in Fig. 3, one can find that the value of the Forster distance measurement for LS277 is 4.5 nm.

Now we need to find the number of LS277 molecules inside one silica nanoparticle to estimate the average distance between them. The number of such molecules can be found from eqn (1), see also eqn (3) of ref. 3. The quantum yield of the encapsulated dye is found to be 1.5% (see the ESI;† note that a possible change of the extinction coefficient (absorptivity) of the dye after encapsulation is assigned to the change of the quantum yield of the encapsulated dye, see the discussion paragraph after eqn (2)). This is ~5 times higher than the one of the free dye. This is presumably due to encapsulation of LS277 in the non-polar (alkane) environment of nanopores of nanoparticles. Therefore, one can estimate the number of LS277 molecules in each NP1_LS277 nanoparticle equal to 415 ± 8. Similarly, each NP2_LS277 nanoparticle has 125 ± 10 molecules of LS277 dye. (It is worth noting that the larger amount of molecules calculated is rather similar to what was reported previously in ref. 2 and 3 for rhodamine 6G dye.) Assuming geometry of cylindrical pores of diameter 3–4 nm and volume of the pores 0.6–0.8 $cm^3\ g^{-1}$ (see ref. 2, 3, 26 and 27 in which similar mesoporous silica was characterized; the pores of this size can be seen in TEM images of Fig. 1), and typical mass density of mesoporous silica,[3,26,28] one can estimate the average distance between LS277 molecules to be 2.3–5.3 nm and 7.5–18 nm in NP1_LS277 and NP2_LS277 particles, respectively. Comparing to the Forster distance, one can conclude that the loading of NP1_LS277 particles is at the limit beyond which the dye starts quenching its fluorescence. The loading of NP2_LS277 particles is substantially below that limit.

It is interesting to compare the brightness of nanoparticles synthesized with the one of commercially available quantum dots which work in a similar IR region, QD800. In contrast to the dye-based silica nanoparticles NP_LS277, quantum dots have a rather broad excitation (absorbance) spectrum. Since we aim at the use of NIR particles for *in vivo* applications, both excitation and emission wavelengths should preferably be within the NIR spectral range, *i.e.*, >700 nm. The largest extinction coefficient of QD800 in the NIR range is at 700 nm, and equals to 300 000 $M^{-1}\ cm^{-1}$ according to the manufacturer specifications. Taking the manufacturer given QY = 50%, one obtains the “brightness” of 150 000 $M^{-1}\ cm^{-1}$ for a single QD800 quantum dot.

Similar calculations can be done for NP_LS277 particles. Using similar calculations, one obtains that the brightness = 620 000 $M^{-1}\ cm^{-1}$ for a single NP1_LS277 particle, and 190 000 $M^{-1}\ cm^{-1}$ for single NP2_LS277 particle. (Note that these values can be found by multiplying the brightness of the particles relative to the brightness of one molecule of LS277 by the brightness of LS277.) Thus, one can conclude that NP1_LS277 is 400% and NP2_LS277 is 27% brighter than QD800 quantum dots. The calculated brightness of LS277 dye, NP1_LS277 and NP2_LS277 nanoparticles, and the commercial quantum dot are listed in Table 1. The relative brightness of these entities is shown in (Fig. 3). It should be noted that this comparison is more instrumental rather than fundamental. Each QD800 dot is 17–20 nm in diameter, which is smaller than our 28 nm nanoparticles. Quantum dots can be noticeably brighter if one uses shorter wavelengths to excite fluorescence. On the other hand, the brightness of quantum dots decreases virtually to zero when the excitation wavelengths of 760–820 nm are used. In the same time, such excitation gives the maximum fluorescent brightness for our fluorescent nanoparticles due to the strong absorption within this NIR window. Thus, one can conclude that we report on the brightest fluorescent particles that have absorbance/ fluorescent in the NIR range.

Table 1 includes the data on life-time of the dye before and after encapsulation in the particles. We have previously shown that the fluorescence lifetime of cyanine dyes, such as LS277, is significantly affected by the polarity of the media.[40] Less polar medium led to a longer lifetime. The lifetime obtained from NP1_LS277 and NP2_LS277 in water is 0.42 and 0.37 ns, respectively. These values were derived from the exponential decay shown in (Fig. 4). Comparing these values with the lifetime of LS277's in water (0.20 ns (ref. 40)), one can conclude that the environment of the encapsulated dye changed presumably for the less polar medium. This is coherent with physical encapsulation of dye molecules inside nanoscale environment created by alkane chains of templating surfactant molecules.

Since the major application of the described nanoparticles is expected to be the imaging of biological objects, we show compatibility of the synthesized particles with the imaging of biological cells. To demonstrate the uptake of the nanoparticles by cells, we used 4T1luc breast tumor cells, which internalize nanoparticles by a nonspecific mechanism. NP2_LS277 particles were used in this study to test the uptake, and to demonstrate that ever less superior nanoparticles (NP1_LS277 particles are about 3.3 times brighter than NP2_LS277) work nicely for cell imaging using the NIR fluorescent excitation and emission.

The cells were prepared for fluorescent imaging as described in the Experimental section. Incubation of cells was done with nanoparticles of 55 pM concentration and with LS277 dye of 7 nM concentration for the same several periods of time. Exceptionally bright fluorescence was observed within 30 minute post-incubation with, requiring only about 4 s exposure (Fig. 5). Comparable exposure time for cells incubated with LS277 dye was almost 10 times longer, indicating a brighter signal attained with the particles. These results demonstrate that our nanoparticles not only produce brighter signal being at 125 times lower molar concentration than LS277 dye, but also show that the particles can be internalized by cells faster than just dye. If the speed was the same, one would expect the particles to show 5 times higher brightness at these concentrations (5 times the difference in the quantum yield and the same optical density of both particle and dye solutions). Longer times shown in Fig. 5 demonstrate approximately this ratio of fluorescence coming from cells incubation with the dye and particles. Longer incubation times were tested as well. Fig. 5 shows that the NIR nanoparticles gave always higher fluorescence.

Fig. 6 shows an exceptionally long stability of the cell samples after the treatment with NP_LS277 particles compared with free LS277 dye. Fig. 6a and c show the images of cells after 24 hours post treatment (done in the way described above) with free dye and nanoparticles, respectively. Fig. 6b and d demonstrates the same measurements with the same exposure times (the exposures are all taken for the same time length of 2 seconds), respectively after 9 weeks post treatment. One can see that the cells treated with the nanoparticles did not lose any brightness, whereas there was no fluorescent signal left for the dye-treated cells.

Conclusion

The synthesis and characterization of ultrabright NIR fluorescent mesoporous silica nanoparticles was presented. LS277 NIR fluorescent dye was physically encapsulated inside

nanochannels of silica nanoparticles. Two types of particles with different concentration of the dye were synthesized NP1_LS277 and NP2_LS277. The dynamic light scattering showed that the sizes of the particles of both types were 28 ± 3 nm. This was confirmed with TEM imaging as well. The wavelengths of the maximum excitation/emission of the particle fluorescence excitation were 804 nm and 815 nm, respectively. Fluorescent brightness of each particle of NP1_LS277 (NP2_LS277) type was equivalent to 2070 ± 40 (650 ± 50) of the brightness of free LS277 dye molecules in water. The quantum yield of the dye increases ~5× after encapsulating (to 1.5%). The extinction coefficient was found to be $\varepsilon = 4.2 \times 10^8$ M^{-1} cm^{-1} and $\varepsilon = 1.3 \times 10^8$ M^{-1} cm^{-1} (at 805 nm) for NP1_LS277 and NP2_LS277 particles, respectively. Using 4T1luc breast tumor cells, we demonstrated that the synthesized particles were internalized by cells faster than free dye, and bring higher fluorescence. After incubation of cells with nanoparticles of 55 pM concentration within 30 minutes, the NIR images are exceptionally bright compared to the cell incubated with LS277 dye of 7 nM concentration for the same period of time. Fluorescent NIR brightness of the cell treated with the described nanoparticles stayed essentially the same even after nine weeks post treatment; whereas no fluorescent signal survived of the cells treated with free LS277 dye.

Experimental

Tetraethyl orthosilicate (TEOS, Aldrich) was used as silica source. Cetyltrimethylammonium chloride (CTAC, 25% aqueous solution, Aldrich) was used for as a structure-directing agent, and triethanolamine (TEA, Aldrich) as an catalyst and gelator. IR820, 4-carboxyphenylboronic acid, and tetrakis(-triphenylphosphine)palladium were purchased from Sigma-Aldrich and used as received. All the chemicals were used without further purification. Ultrapure de-ionized (DI) water from Milli-Q ultrapure system was used for all synthesis, dialysis, and storage steps.

Preparation of fluorescent mesoporous nanoparticles

LS277 fluorescent dye was synthesized as described previously.[41] Molecular structure of this dye is shown in (Fig. 7). The particles were prepared using a protocol which is a modified version of the described in ref. 2. Specifically, the synthesis of fluorescent mesoporous nanoparticles (NP) was based on the use of TEA as an alkaline catalyst. Relative molar composition of 1.0TEOS : 0.2CTACl : 0.0026–0.017LS277 dye : 10.4TEA : 142H_2O was used. The water used was purged with nitrogen gas under stirring for 15 minutes. In a typical synthesis of nanoparticles, TEOS and TEA were mixed in a glass vial and heated for 1 h at 90 °C without stirring. Another solution of mixed LS277, CTAC, and water was kept under stirring for 1 h. These two solutions were mixed in a high-density polypropylene bottle and stirred for 5 h. To extract particles from the synthesizing bath, a regular dialysis method was used. Spectra/Por® RC membrane, (MW of 15 000 Da) was used.

Particles characterization

Particle size distributions and zeta-potential measurements were obtained using a dynamic light scattering (DLS), particle-size analyzer (Brookhaven, NY) equipped with a standard 35

mW diode laser and an avalanche photodiode detector. 0.25 mL of stock solution was diluted to 3 mL with deionized water and ultrasonicated for 5 min prior to particle size measurements. Effective and most probable (mode) diameters presented are the averages of three runs. Fluorescence spectrophotometers Cary Eclipse (Varian. USA), Horiba Fluorelog 3 (Horiba, Japan) were used to measure the fluorescence. UV-2401PC UV-Vis spectrophotometer (Shimadzu, Japan) was used to measure absorbance. Steady-state fluorescence spectra of the free dye and dye encapsulated inside silica nanoparticles were excited at 760 nm and recorded over the range of 760 to 900 nm wavelengths. The integration of fluorescence was done over the range of wavelengths starting from 785 nm (to avoid any contribution from particles' light scattering) to 880 nm. The lifetime of the LS (NP_LS277) and LS277 were measured using a time-correlated single photon counting (TSCPS) technique (Horiba, Japan) with excitation source NanoLed at 773 nm (Horiba) and impulse repetition rate of 1 MHz at 90° to a R928P detector (Hamamatsu Photonic, Hamamatsu, Japan). The detector was set to 815 nm with 20 nm band pass. The multichannel analyzer (MCA) recorded repetitive start-stop signals from the TAC and generated a histogram of photons as a function of time-calibrated channels (0.007 ns per channel) until the peak signal reached 10 000 counts. The lifetime was recorded on a 50 ns scale. The instrument response function was obtained by using Rayleigh scatter of Ludox-40 (Sigma-Aldrich, St. Louis, MO) at 773 nm emission. DAS6 software (Horiba) was used for lifetime calculation. The goodness of the exponential fit was judged by χ^2 values.

Cell culture

4T1luc cells were grown in Dulbecco's Modified Eagle Medium (DMEM) with 10% Fetal Bovine Serum (FBS). Fluorescence microscopy was performed with Olympus BX51 upright microscope. 4′,6-Diamidino-2-phenylindole dihydrochloride (DAPI) was detected with excitation 330–385 nm and emission 420 nm. LS277 fluorescence detected with 775/70 em and 845/55 detection.

Cell fluorescent imaging

Cells were plated in an 8-well chamber slide and allowed to grow overnight. The following day the DMEM growth medium was removed and replaced with the same medium but containing either dye alone (LS277) or nanoparticles (NP2_LS277). 7 nM dye solution and NP2_LS277 particles solution of 55 pM (approximately equivalent optical density of both particles and dye). The first well in each plate was a control – with no dye or nanoparticles. The time course for the remainder was 30 min, 1 h, 2 h, 4 h, and 24 h. At the appropriate time, the medium was removed and the cells were washed once with PBS, PBS was removed and mounting media added. After removal of the chambers, the slide was cover-slipped with Vectashield with DAPI nuclear stain (Vector Laboratories, Burlingame, CA).

Supplementary Material

Refer to Web version on PubMed Central for supplementary material.

Acknowledgements

I.S. acknowledges support of this work by the National Science Foundation (CBET 1242214).

Notes and references

1. Lei J, Wang L and Zhang J, ACS Nano, 2011, 5, 3447–3455. [PubMed: 21446756]
2. Cho E-B, Volkov DO and Sokolov I, Adv. Funct. Mater, 2011, 21, 3129–3135.
3. Cho EB, Volkov DO and Sokolov I, Small, 2010, 6, 2314–2319. [PubMed: 20859948]
4. Gao J, Chen K, Xie R, Xie J, Lee S, Cheng Z, Peng X and Chen X, Small, 2010, 6, 256–261. [PubMed: 19911392]
5. Gao X, Cui Y, Levenson RM, Chung LW and Nie S, Nat. Biotechnol, 2004, 22, 969–976. [PubMed: 15258594]
6. Medintz IL, Uyeda HT, Goldman ER and Mattoussi H, Nat. Mater, 2005, 4, 435–446. [PubMed: 15928695]
7. Eastman PS, Ruan WM, Doctolero M, Nuttall R, De Feo G, Park JS, Chu JSF, Cooke P, Gray JW, Li S and Chen FQF, Nano Lett, 2006, 6, 1059–1064. [PubMed: 16683851]
8. Fritzler MJ, Lupus, 2006, 15, 422–427. [PubMed: 16898176]
9. Gao XH and Dave SR, Bio-Applications of Nanoparticles, 2007, vol. 620, pp. 57–73.
10. Jokerst JV, Raamanathan A, Christodoulides N, Floriano PN, Pollard AA, Simmons GW, Wong J, Gage C, Furmaga WB, Redding SW and McDevitt JT, Biosens. Bioelectron., 2009, 24, 3622–3629. [PubMed: 19576756]
11. Wang L, Zhao W, O'Donoghue MB and Tan W, Bioconjugate Chem, 2007, 18, 297–301.
12. Akers WJ, Berezin MY, Lee H and Achilefu S, J. Biomed. Opt, 2008, 13, 054042. [PubMed: 19021422]
13. Resch-Genger U, Grabolle M, Cavaliere-Jaricot S, Nitschke R and Nann T, Nat. Methods, 2008, 9, 763–775.
14. Hoffmann K, Behnke T, Drescher D, Kneipp J and Resch-Genger U, ACS Nano, 2013, 7, 6674–6684. [PubMed: 23837453]
15. Shibata S, Taniguchi T, Yano T and Yamane M, J. Sol-Gel Sci. Technol, 1997, 10, 263–268.
16. Ow H, Larson DR, Srivastava M, Baird BA, Webb WW and Wiesner U, Nano Lett. , 2005, 5, 113–117. [PubMed: 15792423]
17. Larson DR, Heikal A, Ow H, Srivastava M, Wiesner U, Baird B and Webb WW, Biophys. J, 2003, 84, 586a.
18. Bagwe RP, Yang CY, Hilliard LR and Tan WH, Langmuir, 2004, 20, 8336–8342. [PubMed: 15350111]
19. Wang L and Tan WH, Nano Lett, 2006, 6, 84–88. [PubMed: 16402792]
20. Zhao XJ, Bagwe RP and Tan WH, Adv. Mater, 2004, 16, 173–176.
21. Yang HH, Qu HY, Lin P, Li SH, Ding MT and Xu JG, Analyst, 2003, 128, 462–466. [PubMed: 12790198]
22. Kim S, Pudavar HE and Prasad PN, Chem. Commun, 2006, 2071–2073.
23. Santra S, Zhang P, Wang K, Tapec R and Tan W, Anal. Chem, 2001, 73, 4988–4993. [PubMed: 11681477]
24. Naik SP and Sokolov I, in Nanoparticles: Synthesis, Stabilization, Passivation and Functionalization, ed. Nagarajan R, ACS, 2008, pp. 214–224.
25. Sokolov I, Kievsky Y and Kaszpurenko JM, Small, 2007, 3, 419–423. [PubMed: 17245779]
26. Sokolov I and Volkov DO, J. Mater. Chem, 2010, 20, 4247–4250.
27. Volkov DO, Cho EB and Sokolov I, Nanoscale, 2011, 3, 2036–2043. [PubMed: 21479304]
28. Sokolov I and Naik S, Small, 2008, 4, 934–939. [PubMed: 18581411]
29. Medintz IL, Pons T, Trammell SA, Blanco-Canosa JB, Dawson PE and Mattoussi H, Colloidal Quantum Dots for Biomedical Applications IV, Proc. SPIE 7189, ed. Osinski M, Jovin TM and Yamamoto K, 2009, p. 71890M.
30. Maeda Y, Nishijima H, Akita S, Matsumoto T, Nakayama Y and Kawai T, Jpn. J. Appl. Phys., Part 1, 2001, 40, 1425–1428.
31. Schenkman JB, Jansson I, Lvov Y, Rusling JF, Boussaad S and Tao NJ, Arch. Biochem. Biophys, 2001, 385, 78–87. [PubMed: 11361029]

32. Meyer E, Bennewitz R, Pfeiffer O, Barwich V, Guggisberg M, Schar S, Bammerlin M, Loppacher C, Gysin U, Wattinger C and Baratoff A, in Fundamentals of Tribology and Bridging the Gap Between the Macro- and Micro/Nanoscales, ed. Bhushan B, Springer, Netherlands, 2001, pp. 67–81.
33. Bai MF and Achilefu S, Bioorg. Med. Chem. Lett, 2011, 21, 280–284. [PubMed: 21106373]
34. Zhang Z, Fan J, Cheney PP, Berezin MY, Edwards WB, Akers WJ, Shen D, Liang K, Culver JP and Achilefu S, Mol. Pharmaceutics, 2009, 6, 416–427.
35. Hsu JWP, Manfra MJ, Lang DV, Baldwin KW, Pfeiffer LN and Molnar RJ, J. Electron. Mater, 2001, 30, 110–114.
36. Chan WCW, Maxwell DJ, Gao XH, Bailey RE, Han MY and Nie SM, Curr. Opin. Biotechnol, 2002, 13, 40–46. [PubMed: 11849956]
37. Chan WCW and Nie SM, Science, 1998, 281, 2016–2018. [PubMed: 9748158]
38. Palantavida S, Guz NV, Woodworth CD and Sokolov I, Nanomedicine, 2013, 9, 1255–1262. [PubMed: 23665420]
39. Lakowicz JR, Principles of fluorescence spectroscopy, Springer, New York, 2006.
40. Berezin MY, Lee H, Akers W and Achilefu S, Biophys. J, 2007, 93, 2892–2899. [PubMed: 17573433]
41. Lee H, Mason JC and Achilefu S, J. Org. Chem, 2006, 71, 7862–7865. [PubMed: 16995699]

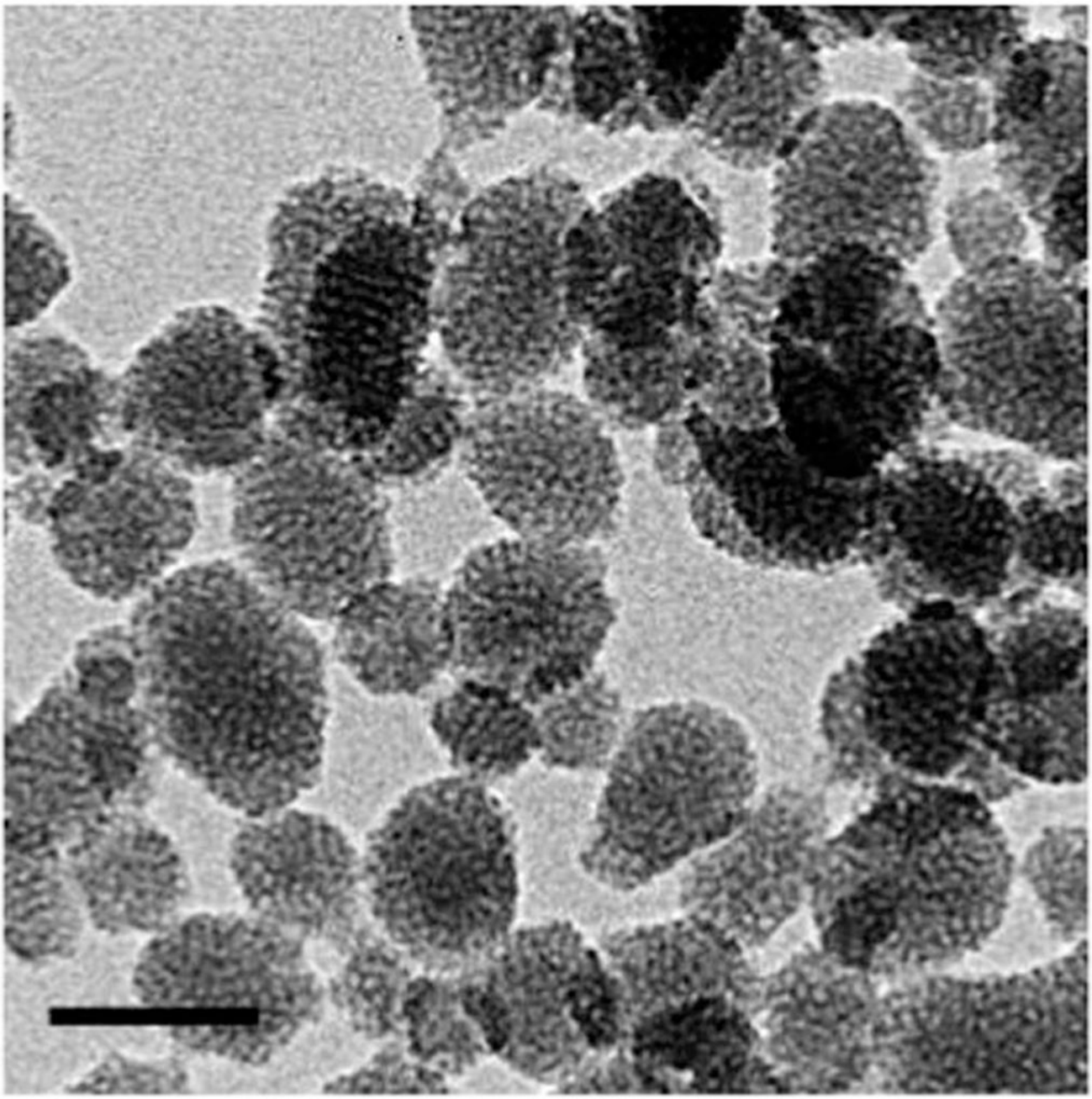

Fig. 1.
TEM image of fluorescent mesoporous silica nanoparticles. The bar size is 50 nm.

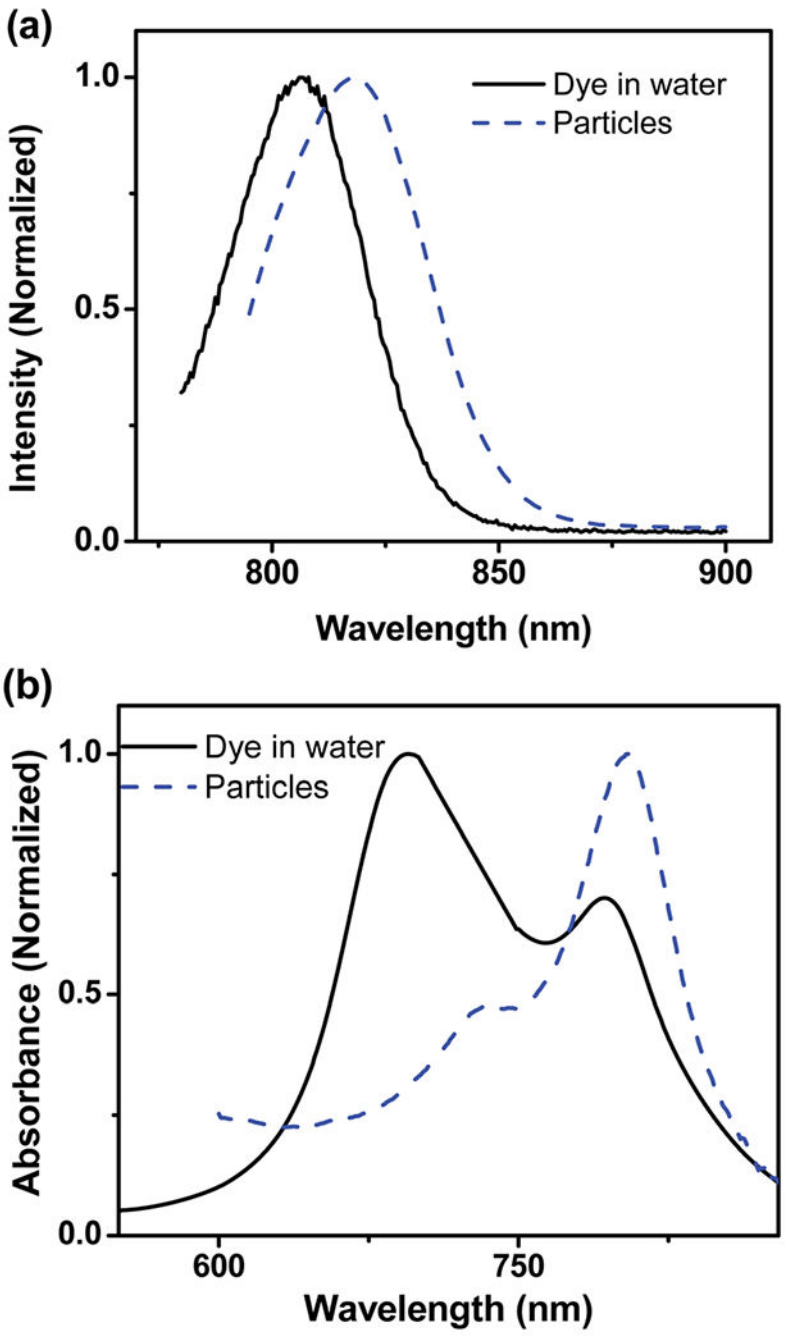

Fig. 2.

Representative absorbance and fluorescent spectra of the synthesized nanoparticles and free dye in water. (a) Fluorescent spectrum of particles and LS277 dye in water. (b) Absorbance spectrum of particles and LS277 dye in water.

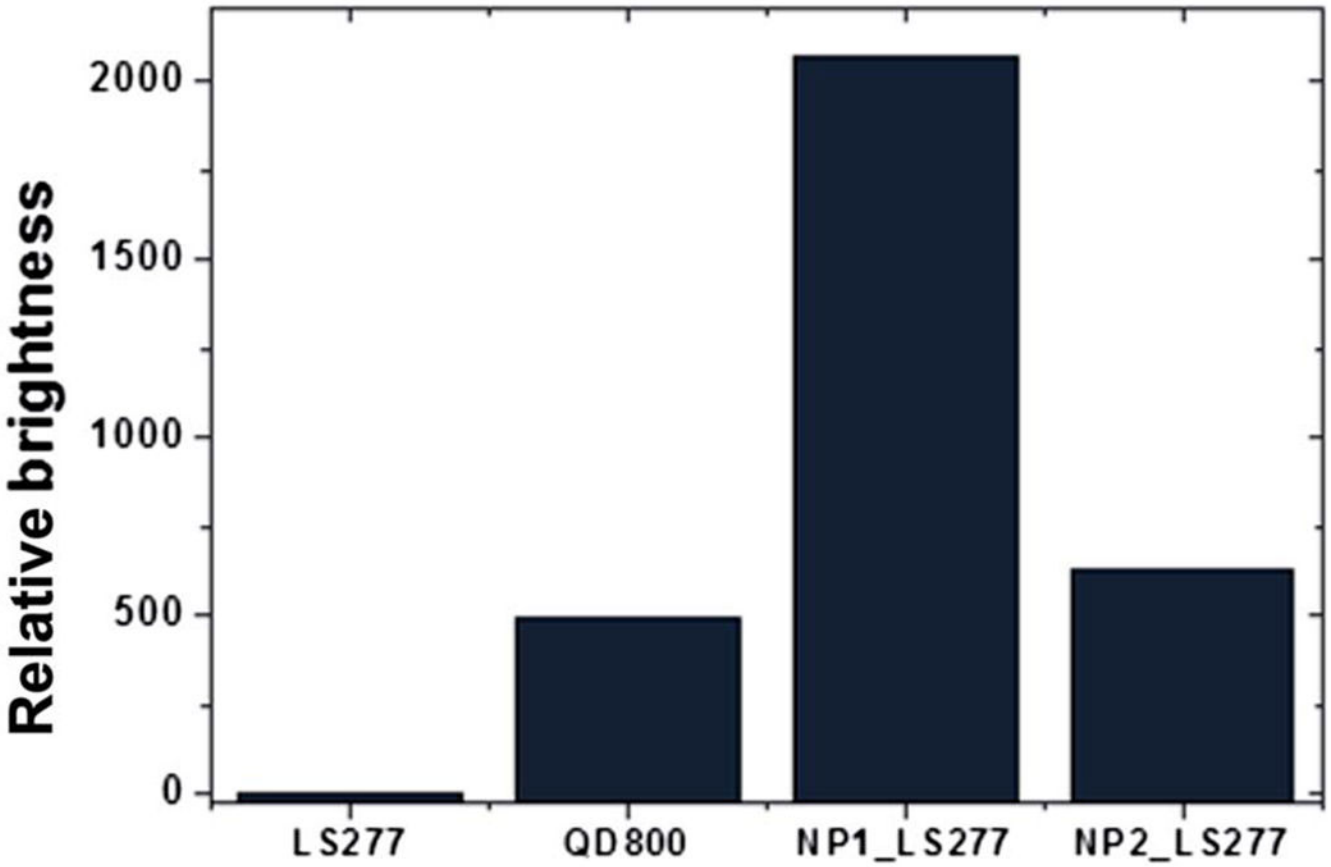

Fig. 3.

Relative fluorescent brightness in the NIR range of single LS277 molecules, QD800 quantum dot, and ultra-bright silica particles described in this work (NP1_LS277 and NP2_LS277).

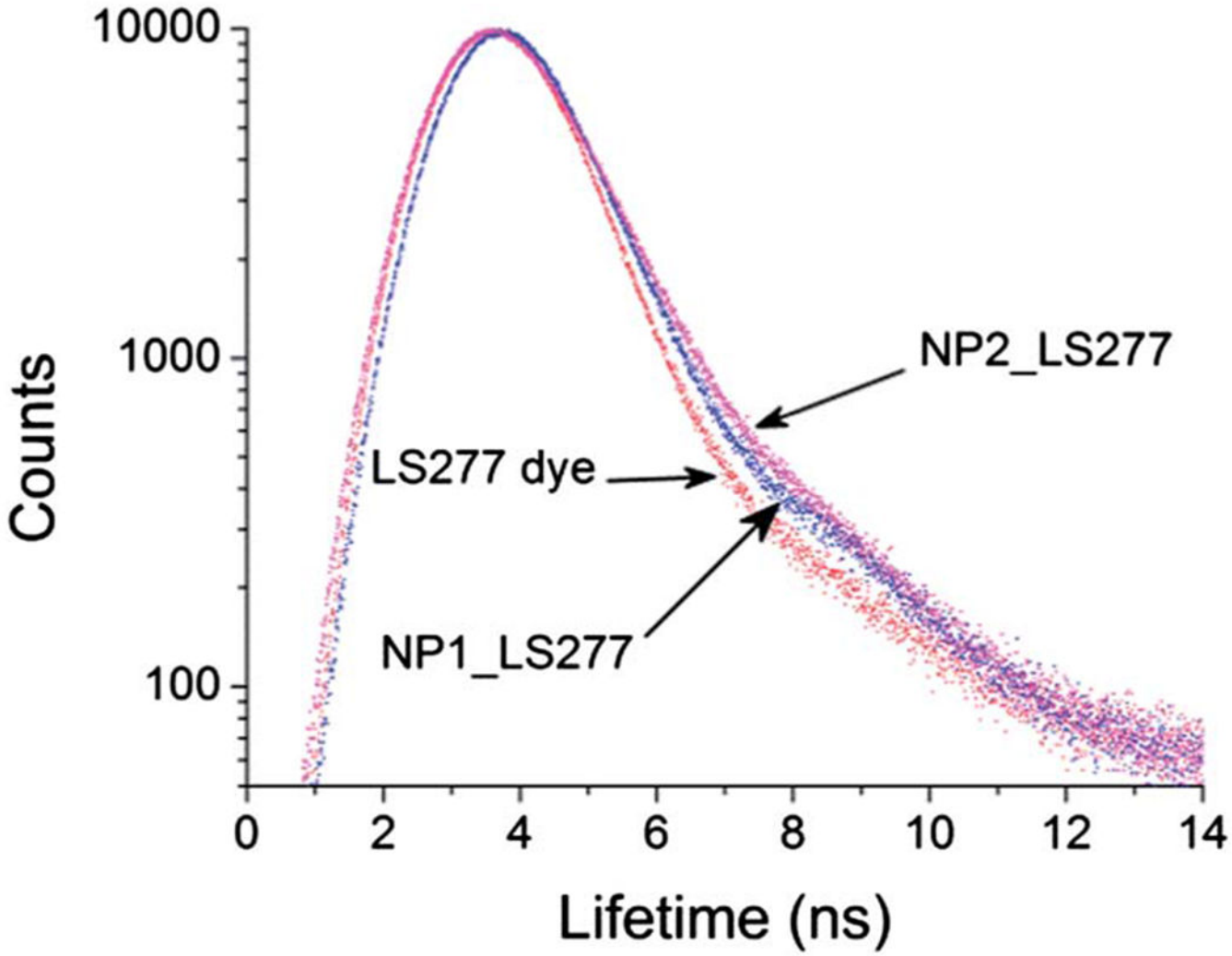

Fig. 4.
Decay profiles of fluorescence lifetime of LS277, SiNP1_LS277 and SiNP2_LS277.

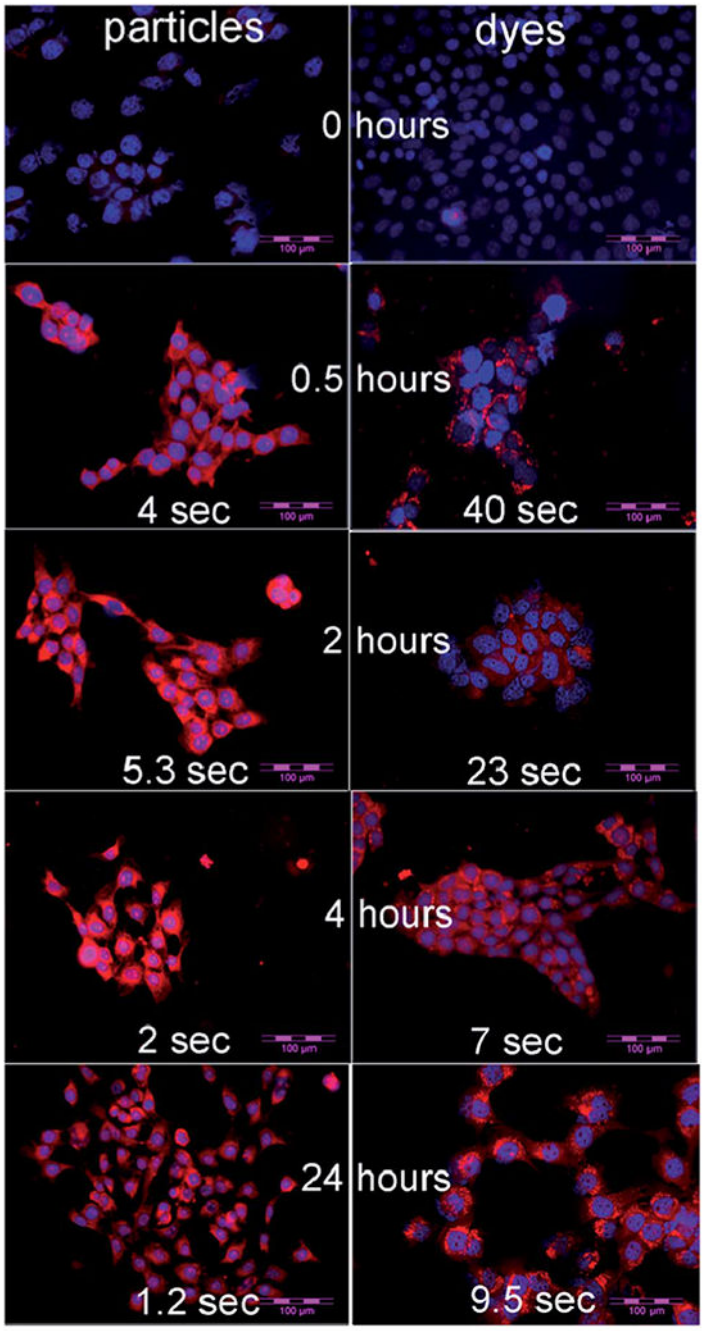

Fig. 5.

NIR fluorescent images of 4T1luc tumor cells. Left column is the cells treated with NP2_LS277 particles. Right with column is the cells treated with LS277 dye. Both fluorophores were used at the same molar concentration. The treatment time is shown at the middle of particle–dye pairs. The exposure times (assigned automatically by the camera) are shown at the bottom of each image. Scale bar: 100 μm.

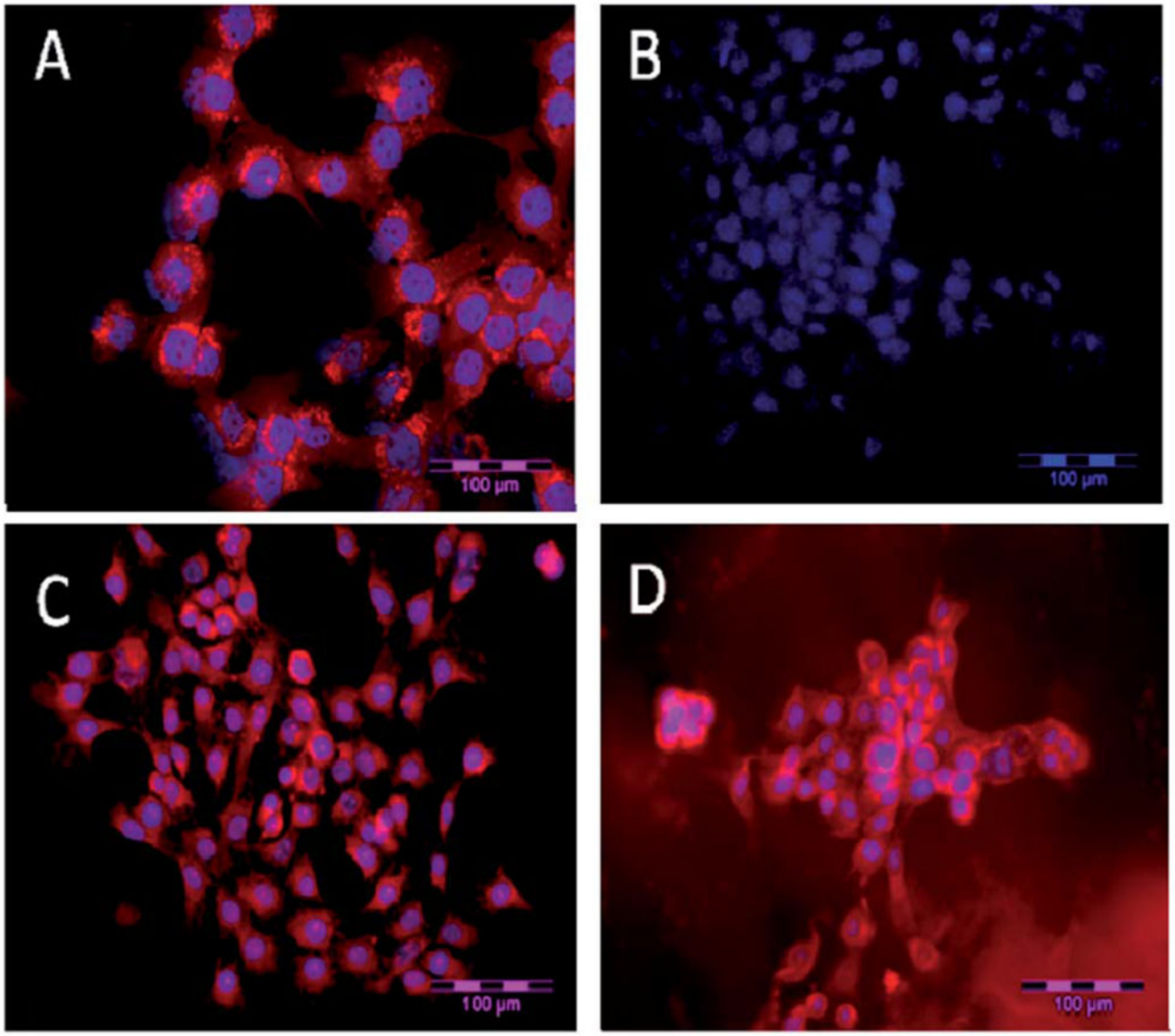

Fig. 6.

A long-term stability of the cell sample. NIR fluorescence microscopy of 4T1luc tumor cells. (A) Cells 24 h post treatment with LS277 dye; (B) re-imaging of cells shown in (A) after 9 weeks; (C) cells 24 h post treatment with NP2_LS277 particles; (D) re-imaging of cells shown in (C) after 9 weeks; red: NIR fluorescence; blue: DAPI nuclear stain; scale bar 100 μm.

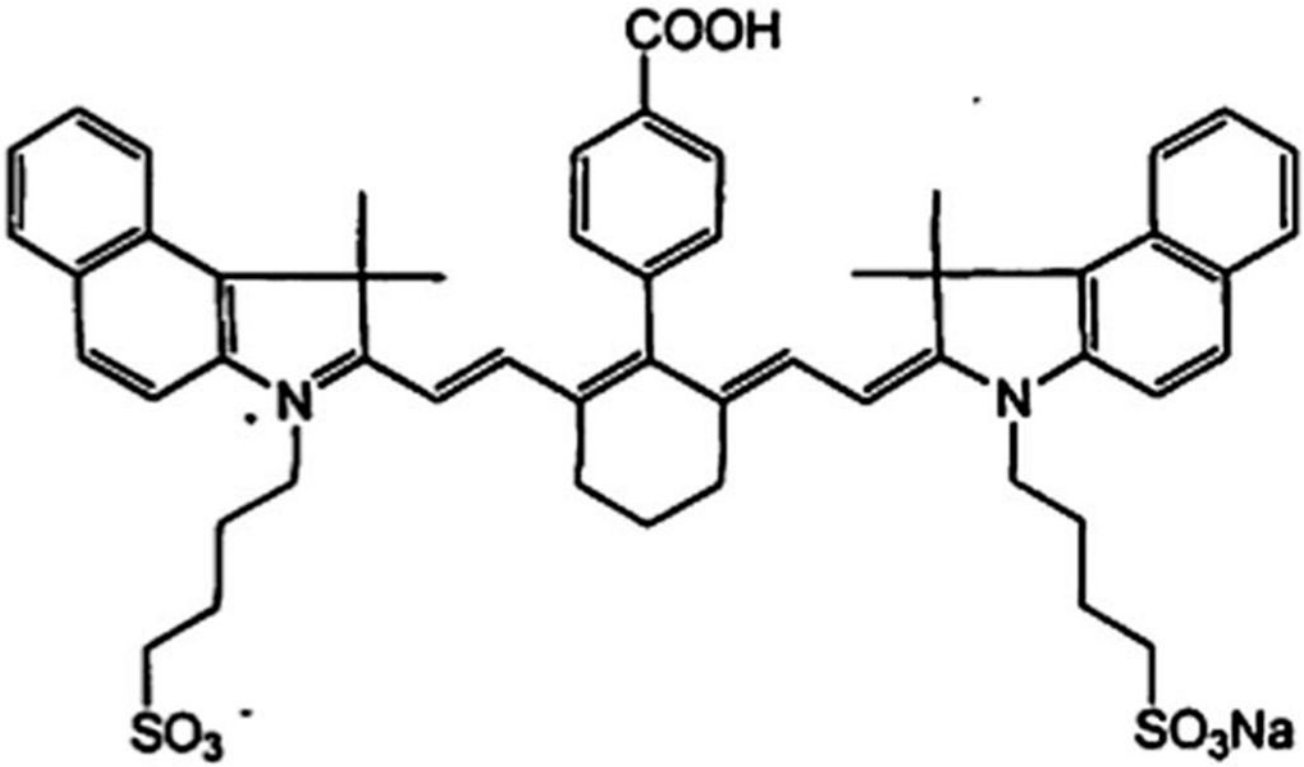

Fig. 7.
Molecular structure of LS277 dye.

Table 1

Extinction coefficient, quantum yield, lifetime and brightness of LS277, SiNP1_LS277, SiNP2_LS277 and QD800 sample from Invitrogen

Materials	Extinction coefficient, [M^{-1} cm^{-1}]	Quantum yield	Brightness, [M^{-1} cm^{-1}]	Lifetime [ns]
LS277	100 000	0.003	3000	0.20
SiNP1_LS277	41 500 000	0.015	620 000	0.42
SiNP2_LS277	12 500 000	0.015	190 000	0.37
QD800	300 000	0.5	150 000	>10